
Proceedings Paper:
Kent, JT orcid.org/0000-0002-1861-8349, Hussein, I and Jah, MK (2016) Directional Distributions in Tracking of Space Debris. In: 2016 19th International Conference on Information Fusion Proceedings. 2016 19th International Conference on Information Fusion (FUSION), 05-08 Jul 2016, Heidelberg, Germany. International Society of Information Fusion , pp. 2081-2087. ISBN 978-0-9964-5274-8

Directional Distributions in Tracking of Space Debris

John T Kent
Department of Statistics
University of Leeds
Leeds LS2 9JT, UK
Email: j.t.kent@leeds.ac.uk

Islam Hussein
Applied Defense Solutions
10440 Little Patuxent Parkway, Suite 600
Columbia, MD 21044, USA
Email: ihussein@applieddefense.com

Moriba K Jah
College of Engineering
Office for Research & Discovery
The University of Arizona
Tucson, AZ 85721, USA
Email: moribajah@email.arizona.edu

***Abstract*—Directional distributions play an important role in describing uncertainty in spherical coordinates. A review is given of some standard distributions on the sphere which arise as special cases of the Fisher-Bingham distribution. A new distribution, called the "extreme FB5" distribution, is introduced to describe semi-concentrated behavior on the sphere, that is, patterns of data that are unimodal and concentrated near a great circle. This behavior is particularly relevant to tracking problems. Properties of the new distribution are discussed and methods are given for simulation and estimation. Two simple error propagation illustrations are given to demonstrate the usefulness of the new model.**

I. Introduction

Methods for directional distributions are becoming increasingly important in space tracking and related applications [1]. Conventionally approximate Euclidean coordinates have often been used on the sphere, but severe distortions can occur in certain circumstances. The motivation for this work is to improve the representation of the state uncertainties of space objects and to improve the prediction of the locations of these objects after some user-defined time interval.

Current methods of space object tracking, based upon angles-only data have two main limitations: (a) the angular errors are modelled as i.i.d. Gaussian, and (b) the estimation of the space object trajectory assumes the angular data constitute proper vector measurements in Euclidean space. Neither of these assumptions is actually true, though for small errors, the assumptions have been shown to be approximately valid.

Two major challenges in space object tracking are (a) the ability to accurately associate space object detections with unique space objects and (b) the ability to accurately predict where any space object will be as a function of time. The work presented here attempts to demonstrate that representing the angular uncertainty on the sphere, as opposed to treating it as a Euclidean vector, yields more precise estimates and predictions for space object state error uncertainty. This in turn aids in space object data and track association, especially as the number of simultaneous detections increases.

Uncertainty propagation has been investigated in detail in orbital debris research, particularly in how it applies to collision probability computation and Bayesian estimation. Junkins, Akella, and Alfriend [2] studied the general problem of non-linear error propagation in orbital mechanics and showed that the choice of coordinates has a significant impact on how fast errors become non-Gaussian. Fujimoto, Scheeres, and Alfriend [3] developed analytical techniques to propagate uncertainty in the two-body problem using the concept of state transition tensors. Aristoff, Horwood, and Poore [4], [5] discussed the use of implicit Runge-Kutta methods and the Gauss von Mises distribution to better capture the evolution of the orbit uncertainty in angular coordinates. Valli et al. [6] derived a method for nonlinear propagation of uncertainty in celestial mechanics based on differential algebra. Several authors [7], [8], [9], [10] have investigated the use of Gaussian mixture models for uncertainty propagation and Bayesian estimation. However, the majority of this research has been focused on propagating uncertainty in Cartesian or orbital element coordinates, ignoring the directional nature of the space orbital debris tracking problem.

In this paper we review and illustrate the use of various special cases of the Fisher-Bingham distribution on the sphere. In particular, we propose a new version of this distribution which is more appropriate in the semi-concentrated setting. We describe its basic properties, methods of estimation and simulation, and give two examples to illustrate its potential importance in tracking problems.

II. Fisher-Bingham distributions

The Fisher-Bingham distribution on the unit sphere $S_2 = \{\boldsymbol{x} \in \mathbb{R}^3 : \boldsymbol{x}^T\boldsymbol{x} = 1\}$ in $\mathbb{R}^3$ is an important distribution. In its most general form, it has probability density

$$f(\boldsymbol{x}) \propto \exp\{\boldsymbol{\nu}^T\boldsymbol{x} + \boldsymbol{x}^T A\boldsymbol{x}\}$$

with respect to the uniform distribution on the sphere, $\mu(d\boldsymbol{x})$, say. If $\boldsymbol{x}$ is written in polar coordinates $x_1 = \sin\theta\cos\phi,\ x_2 = \sin\theta\sin\phi,\ x_3 = \cos\theta$, where $\theta \in [0, \pi]$ denotes the colatitude and $\phi \in [0, \pi)$ denotes the longitude, then the uniform measure takes the form $\mu(d\boldsymbol{x}) = \sin\theta\, d\theta\, d\phi/(4\pi)$. When the density is used in integration, the notation $f(\boldsymbol{x})\,\mu(d\boldsymbol{x})$ is shorthand for $f(\boldsymbol{x})\,\sin\theta d\theta\, d\phi/(4\pi)$. However, working in Euclidean coordinates is generally more insightful than working in polar coordinates.

The parameters of the density are the vector $\boldsymbol{\nu}(3 \times 1)$ and the symmetric matrix $A(3 \times 3)$. It is often convenient to write $\boldsymbol{\nu} = \kappa\boldsymbol{\nu}_0$ where $\kappa > 0$ is a concentration parameter and $\boldsymbol{\nu}_0$ is

a unit 3-vector. The parameter matrices A and $A + \lambda I$ define the same density since $\lambda \boldsymbol{x}^T \boldsymbol{x} = \lambda$ is constant and can be absorbed in the normalizing constant. For the purposes of this paper, the normalizing constants will be suppressed with the "proportional to" ($\propto$) notation.

The full Fisher-Bingham distribution has 8 parameters and can be denoted FB8. However, the parameters cannot be easily interpreted; hence it is helpful to consider restrictions on the parameters. Important special cases include the following.

- The Fisher distribution, $A = 0$ (also known as the von Mises-Fisher distribution when the dimension of the sphere is allowed to be more general). If we write $\boldsymbol{\nu} = \kappa \boldsymbol{\nu}_0$ where $\kappa \geq 0$ and $\boldsymbol{\nu}_0$ is a unit vector, then this distribution has concentration parameter κ and (provided $\kappa > 0$) modal direction $\boldsymbol{\nu}_0$. The density is invariant under rotations of the sphere about the $\boldsymbol{\nu}_0$ axis. Hence it can be described as "isotropic". Under high concentration it behaves as an isotropic bivariate normal distribution in the tangent plane to the sphere at the modal direction.
- The Bingham distribution ($\boldsymbol{\nu} = 0$). This density has antipodal symmetry ($f(\boldsymbol{x}) = f(-\boldsymbol{x})$) and so is useful for modelling axes (= unsigned directions). Let $A = \Gamma \Lambda \Gamma^T$ be the spectral decomposition of A. Here $\Lambda = \text{diag}(\lambda_{\text{max}}, \lambda_{\text{mid}}, \lambda_{\text{min}})$ contains the eigenvalues in decreasing order, and the columns of the 3×3 orthogonal matrix $\Gamma = \begin{bmatrix} \boldsymbol{\gamma}_{(\text{max})} & \boldsymbol{\gamma}_{(\text{mid})} & \boldsymbol{\gamma}_{(\text{min})} \end{bmatrix}$ contain the corresponding eigenvectors. Without loss of generality, the eigenvalues may be shifted by a common value without affecting the distribution. Two common special cases, both characterized by a concentration parameter $\beta > 0$, are the bimodal case ($\lambda_{\text{max}} = \beta > \lambda_{\text{mid}} = \lambda_{\text{min}} = 0$) with the mode along the $\pm\boldsymbol{\gamma}_{(\text{max})}$ axis, and the girdle case ($\lambda_{\text{max}} = \lambda_{\text{mid}} > \lambda_{\text{min}} = -\beta$) with the mode at all points on the great circle perpendicular to the $\pm\boldsymbol{\gamma}_{(\text{min})}$ axis. The Bingham distribution can also exhibit intermediate behavior.
- The "aligned" Fisher-Bingham distribution (FB6). This is a 6-parameter sub-family of FB8, obtained when $\boldsymbol{\nu}_0$ equals one of the eigenvectors of A. It is still has too many parameters for the parameters to be easily interpreted, but it forms the basis for the following two special cases.
- The "balanced" 5-parameter Fisher-Bingham distribution, FB5b (also known as the Kent or Fisher-Bingham-Kent distribution) [11]. The FB5b distribution is a special case of FB6 where $\boldsymbol{\nu} = \boldsymbol{\gamma}_{(\text{mid})}$ and where $\lambda_{\text{max}} = \beta,\ \lambda_{\text{mid}} = 0,\ \lambda_{\text{min}} = -\beta$, for some $\beta \geq 0$. The adjective "balanced" has been added to the name here to distinguish this distribution from another 5-parameter choice given below. Write κ as κ_b for clarity in this setting. Provided $\kappa_b \geq 2\beta$, the density has a mode in the $\boldsymbol{\nu}$ direction. The contours of constant probability are oval-shaped with the major axis pointing along the $\boldsymbol{\gamma}_{(\text{mid})}$ axis and the minor axis pointing along the $\boldsymbol{\gamma}_{(\text{min})}$ axis. Under high concentration the distribution is approximately bivariate normal and concentrated near the modal direction $\boldsymbol{\nu}$.
- The new distribution introduced in this paper can be called the "extreme" 5-parameter Fisher-Bingham distribution, FB5e. The FB5e distribution is another special case of FB6, but is better suited to describing unimodal data concentrated near a great circle. In this case $\boldsymbol{\nu} = \boldsymbol{\gamma}_{(\text{max})}$ with $\lambda_{\text{max}} = \lambda_{\text{mid}} = 0 \geq \lambda_{\text{min}} = -\delta$. Write κ as κ_e in this setting for clarity. This distribution can be viewed as a combination of a Fisher and a girdle Bingham, where the mode of the Fisher lies on the great circle mode of the Bingham.

The next section will discuss in more detail the properties of FB5e and give a comparison to FB5b.

III. Further details about the FB5b and FB5e distribution

A. High concentration

To study the asymptotic bivariate normal behavior of any unimodal distribution on the sphere under high concentration, it suffices to take a second order Taylor series of the log density in tangent coordinates at the modal direction. Then the 2×2 second derivative matrix represents the inverse covariance matrix. We shall investigate this limiting behavior for the FB5b and FB5e distributions.

B. Behavior of the FB5b distribution

The FB5b distribution is unimodal, provided $2\beta/\kappa_b \leq 1$. The easiest way to see this property is to follow every line of longitude from the mode (at the north pole, say) to the south pole and to note that the probability density is decreasing on these lines.

On the other hand, if $2\beta/\kappa_b > 1$, the FB5b density has two equal modes equi-spaced about $\boldsymbol{\nu}_0$, a bit like two rabbit ears. Such behavior is generally unappealing, thus limiting the usefulness of the distribution in such cases.

Next consider the high concentration behavior. That is, let κ_b get large with the ratio $2\beta/\kappa_b < 1$ held fixed. The inverse variance matrix of the limiting bivariate normal distribution (with an appropriate orientation for the coordinates in the tangent plane) takes the form

$$\Sigma^{-1} = \begin{bmatrix} \kappa_b - 2\beta & 0 \\ 0 & \kappa_b + 2\beta \end{bmatrix}.$$

C. Behavior of the FB5e distribution

The dependence of FB5e on δ is different from the dependence of FB5b on β. In particular, for any choice of $\delta \geq 0$, the FB5e density is unimodal with the mode in the direction $\boldsymbol{\nu}_0$.

Under high concentration, FB5e mimics the bivariate normal distribution, just as FB5b. However, the formula for the inverse covariance matrix is different. For FB5e, the inverse covariance matrix takes the form

$$\Sigma^{-1} = \begin{bmatrix} \kappa_e & 0 \\ 0 & \kappa_e + 2\delta \end{bmatrix}.$$

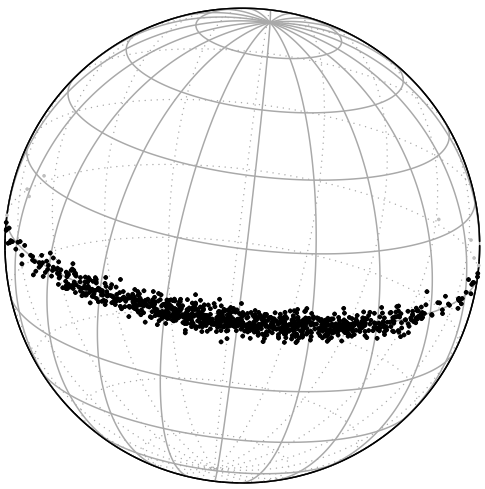

Fig. 1. Simulation results for FB5e with parameters $\kappa_e = 4,\ \delta = 500$. Points on the front half of the sphere are plotted in black; points on the back in gray.

The FB5e density is better able than FB5b to describe data which lie very near a great circle, but whose projection onto the great circle have a unimodal distribution (in fact an approximate von Mises distribution). Fig. 1 with $\kappa_e = 4,\ \delta = 500$ shows a random sample from an FB5e density. The mode lies on the equator and the data are tightly clustered near the equator. The range of the data along the equator roughly fills a semicircle. It is not possible to create this pattern with the FB5b distribution.

D. Confounding

As argued above, the FB5e distribution provides a useful alternative to FB5b in the semi-concentrated case. However, when the ellipticity is not too extreme, both models can be used to describe a dataset, and there will be little difference between the two models. That is, the question of model choice is important in certain settings, and irrelevant in others. A more systematic study is needed to be more precise in these conclusions.

IV. Simulation issues

A powerful new simulation methodology for Fisher-Bingham distributions has recently been developed [12]. The basis for the methodology is an acceptance/rejection technique for the Bingham distribution using an angular central Gaussian (ACG) envelope.

The ACG distribution is straightforward to describe and to simulate on the unit sphere in p-dimensional Euclidean space, for any $p \geq 2$. Let Σ be a positive definite covariance matrix and let $\boldsymbol{Y} \sim N_p(0, \Sigma)$ denote a p-variate normal random vector with mean 0 and covariance matrix Σ. Set $\boldsymbol{X} = \boldsymbol{Y}/||\boldsymbol{Y}||$, where $||\boldsymbol{Y}||^2 = \sum_{j=1}^{p} Y_j^2$, to be the projection of $\boldsymbol{Y}$ onto the unit sphere. Then the distribution of Y is called the angular central Gaussian distribution. Its probability density function is given by

$$f_{\text{ACG}}(\boldsymbol{x}) = \frac{|\Sigma|^{-1/2}}{(\boldsymbol{x}^T\Sigma^{-1}\boldsymbol{x})^{p/2}}$$

(with respect to the uniform distribution on the sphere) [13], [14]. By a suitable choice of Σ for a given concentration matrix A for a Bingham distribution, it is possible to ensure efficiency of at least 52% (i.e. an average of not more than $1/0.52 \approx 2$ simulations from the ACG envelope are needed for each accepted value from the Bingham distribution).

Further this simulation method can be extended to the Fisher-Bingham distributions. The inequality $(1-t)^2 \geq 0$ for all real t leads to the bound

$$\kappa t \leq \frac{\kappa}{2} + \frac{\kappa}{2}t^2$$

for all $\kappa \geq 0$ and means that the general Fisher-Bingham density can be bounded above by a multiple of the Bingham density,

$$\exp\{\kappa \boldsymbol{x}^T\boldsymbol{\nu}_0 + \boldsymbol{x}^T A\boldsymbol{x}\} \leq \exp\{\kappa/2 + \boldsymbol{x}^T A^{(0)}\boldsymbol{x}\},$$

where $t = \boldsymbol{x}^T\boldsymbol{\nu}_0$ and $A^{(0)} = (\kappa/2)\boldsymbol{\nu}_0\boldsymbol{\nu}_0^T + A$, and in turn the Bingham density can be bounded by the ACG density. When the Fisher-Bingham distribution is aligned and unimodal (which includes FB5b with $2\beta/\kappa_b \leq 1$ and FB5e for all $\kappa_e \geq 0$ and $\delta \geq 0$), we expect the efficiency of the simulation method to be reasonably efficient at all levels of concentration. A simple simulation study shows that the lowest efficiency for FB5e is about 26% when κ_e is large, whatever the value of δ, and is higher for small values of κ_e.

Similar considerations apply to FB5b. However, for FB5b, there is also a more efficient purpose-built simulation procedure [15], [16].

V. Estimation

Maximum likelihood estimation is awkward for the FB8 distribution because the normalizing constant is difficult to compute efficiently. However, for certain subfamilies of FB8 maximum likelihood estimation is much more tractable. Cases where tractable formulations for the normalizing constant are available include the Fisher, Bingham and FB5b cases [11], [17]. A tractable formulation for FB5e is still to be worked out.

But due to recent developments, there is now a tractable alternative to maximum likelihood estimation for all versions of the FB8 distribution. In [18] the score matching estimator of [19], [20] has been adapted to exponential family models on the sphere. The new estimator depends just on sample moments of the data and is quick and easy to compute. Numerical evidence suggests it generally has good efficiency compared to the maximum likelihood estimator.

Here is a sketch of the main steps for for FB5b and FB5e, starting from a dataset of unit vectors $\boldsymbol{x}_i,\ i = 1, \ldots, n$. The first two steps are the same as in [11].

(a) Find the mean direction $\overline{\boldsymbol{x}}_0 \propto \sum \boldsymbol{x}_i$, where $\overline{\boldsymbol{x}}_0$ is scaled to be a unit vector. Find a 3×3 rotation R_1, say, taking $\overline{\boldsymbol{x}}_0$

to a unit vector along the first coordinate axis, $R_1^T \overline{\boldsymbol{x}}_0 = \overline{\boldsymbol{y}}_0 = \begin{bmatrix} 1 & 0 & 0 \end{bmatrix}$, say. Let $\boldsymbol{y}_i = R_1^T \boldsymbol{x}_i,\ i = 1, \ldots, n$.

(b) Let $S_y = n^{-1} \sum \boldsymbol{y}_i \boldsymbol{y}_i^T$ denote the second moment matrix for the $\{\boldsymbol{y}_i\}$. Find a second rotation

$$R_2 = \begin{bmatrix} 1 & 0 & 0 \\ 0 & c & s \\ 0 & -s & c \end{bmatrix},$$

where $c = \cos\psi,\ s = \sin\psi$, for some angle ψ, so that $(S_z)_{23} = (S_z)_{32} = 0$ and $(S_z)_{22} > (S_z)_{33}$ where we set $\boldsymbol{z}_i = R_2^T \boldsymbol{y}_i$ and $S_z = n^{-1} \sum \boldsymbol{z}_i \boldsymbol{z}_i^T$ is the second moment matrix for the $\boldsymbol{z}_i$. That is, we have diagonalized the lower 2×2 block of S_y. Then the estimates of the 3 principal axes of the original $\boldsymbol{x}_i$ data are the columns of $R_1 R_2$. Similarly the estimates of the 3 principal axes of the transformed $\boldsymbol{z}_i$ data are the three coordinate axes.

(c) The key step in the estimation procedure is the estimation of κ_b and β (or κ_e and δ, respectively). In each case a two dimensional set of linear equations is set up where the coefficients involve second and fourth moments of the Euclidean coordinates of the rotated data $\boldsymbol{z}_i = (z_{i1}, z_{i2}, z_{i3})^T,\ i = 1, \ldots, n$.
For FB5b the density in $\boldsymbol{z} = (z_1, z_2, z_3)^T$ coordinates takes the form

$$f(\boldsymbol{z}) \propto \exp\{\kappa_b z_1 + \beta(z_2^2 - z_3^2)\}.$$

From the data, define a 2-vector $\boldsymbol{d}^{(b)}$ with entries

$$d_1^{(b)} = 2 \sum z_{i1}, \quad d_2^{(b)} = 6 \sum (z_{i2}^2 - z_{i3}^2),$$

and a 2×2 matrix $W^{(b)}$ with entries

$$\begin{aligned} w_{11}^{(b)} &= \sum (1 - z_{i1}^2), \\ w_{12}^{(b)} &= w_{21}^{(b)} = -2 \sum \{z_{i1}(z_{i2}^2 - z_{i3}^2)\}, \\ w_{22}^{(b)} &= 4 \sum \{z_{i2}^2 + z_{i3}^2 - (z_{i2}^2 - z_{i3}^2)^2\}, \end{aligned}$$

where all the sums are over $i = 1, \ldots, n$. Then the parameter estimates are

$$\begin{bmatrix} \hat{\kappa}_b \\ \hat{\beta} \end{bmatrix} = (W^{(b)})^{-1} \boldsymbol{d}^{(b)}.$$

For FB5e a similar set of computations is needed. The density in $\boldsymbol{z}$ coordinates takes the form

$$f(\boldsymbol{z}) \propto \exp\{\kappa_e z_1 - \delta z_3^2\}.$$

From the data, define a 2-vector $\boldsymbol{d}^{(e)}$ with entries

$$d_1^{(e)} = 2 \sum z_{i1}, \quad d_2^{(e)} = 6 \sum (\frac{1}{3} - z_{i3}^2),$$

and a 2×2 matrix $W^{(e)}$ with entries

$$\begin{aligned} &w_{11}^{(e)} = \sum (1 - z_{i1}^2), \quad w_{12}^{(e)} = w_{21}^{(e)} = 2 \sum z_{i1} z_{i3}^2, \\ &w_{22}^{(e)} = 4 \sum (z_{i3}^2 - z_{i3}^4). \end{aligned}$$

Then the parameter estimates are

$$\begin{bmatrix} \hat{\kappa}_e \\ \hat{\delta} \end{bmatrix} = (W^{(e)})^{-1} \boldsymbol{d}^{(e)}.$$

Care is needed in the numerical formulation of these equations in the setting of high concentration.

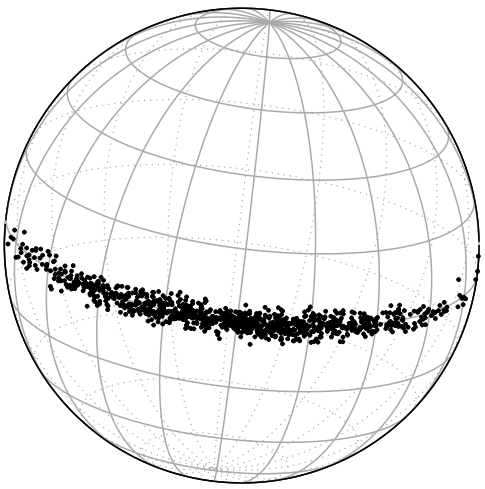

Fig. 2. Example 1. Final positions of a point cloud after error propagation.

VI. Error propagation

A. Example 1

Here is a simple toy example to demonstrate the usefulness of the new FB5e distribution. Consider an observer (at the center of a transparent earth) making an observation on the position and velocity of a space object. The object is known to be in a circular orbit. Further suppose the velocity is measured less accurately than the position. The objective is to predict the object position at a later point in time.

To model this situation we use skew symmetric matrices to generate rotation matrices. If

$$S = \begin{bmatrix} 0 & s_{12} & -s_{13} \\ -s_{12} & 0 & s_{23} \\ s_{13} & -s_{23} & 0 \end{bmatrix},$$

is skew symmetric, then the matrix exponential

$$G = \exp(S) = I + (\sin\theta) S_0 + (1 - \cos\theta) S_0^2$$

is a rotation matrix. Here $\theta = (s_{12}^2 + s_{13}^2 + s_{23}^2)^{1/2})$ and $S_0 = S/\theta$. The elements of S are measured in radians.

For our purposes we use two random rotation matrices based on skew symmetric matrices. For S_A, suppose $s_{12} = 0$ and that s_{13} and s_{23} are independent $N(0, 0.001)$ random variables, that is, mean 0 and variance 0.001. For S_B suppose that $s_{13} = 0$ and that $s_{23} \sim N(0, .001)$ and $s_{12} \sim N(4\pi, 0.25)$ are independently normally distributed. Then G_A represents the effect of perturbing the current location of the object from the north pole and G_B represents the motion of the object (shifted to the north pole) after one unit of time. Let the vector given by the first column of $G_A G_B$ denote the position of the object at one time step into the future. If there were no errors, the

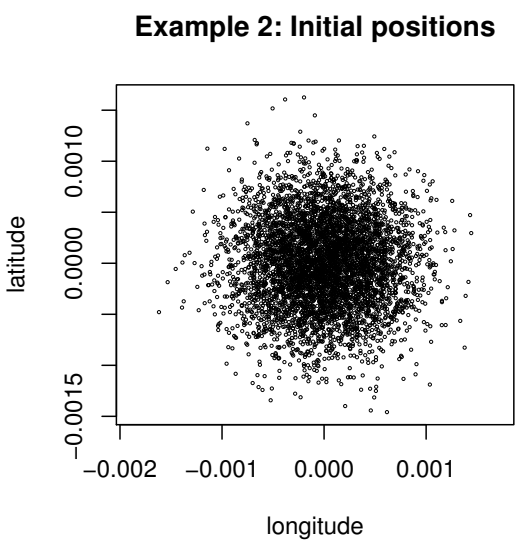

Fig. 3. Example 2. Initial positions of a cloud of points, with latitude and longitude given in degrees.

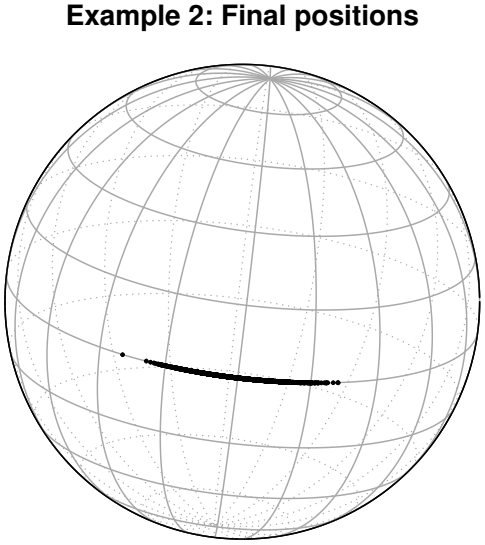

Fig. 4. Example 2. Final positions of a cloud of points. The points lie close to, but not exactly on, the equator.

object would make two orbits of the earth ($4\pi = 2 \cdot 2\pi$) and return to its current position at the north pole.

A plot of 1000 simulated points under this model is given in Fig. 2, where for presentational purposes the mode has been moved to the equator. Comparing this figure to Fig. 1 confirms visually that the FB5e distribution provides a useful description.

B. Example 2

Next, we consider a more realistic space debris problem where we wish to map the uncertainty in an object's trajectory down to the surface of a sphere. A potential application would be the future prediction of an object's pointing direction with respect to a terrestrial sensor. In this example, a space object is in a zero-inclination circular orbit located nominally 400km below the geosynchronous (GEO) orbit. We assume that the object has an initial Gaussian distribution with a standard deviation of 100 km in position and 2 m/s in velocity (assumed uniform in all three directions). Then 5000 particles drawn from the initial distribution were propagated for 14 sidereal days. The particle clouds pre- and post-propagation were projected onto the sphere and each data set was used to estimate a pre- and post-propagation FB5e based on the score matching estimator. The resulting pre- and post-distributions have the following set of estimated parameters:

$$\begin{aligned} \text{Initial estimates:} \quad & \hat{\kappa}_e = 1.69e10, \qquad \hat{\dot{\delta}} = 0.05e10, \\ \text{Final estimates:} \quad & \hat{\kappa}_e = 68.0, \qquad\quad \hat{\dot{\delta}} = 2.67e6. \end{aligned}$$

For visualization, both clouds of points have been rotated to be centered on the equator at the "Greenwich Meridian". The plots are given in Figures 3 and 4. The initial cloud is highly concentrated near a single point on the sphere; hence a blow-up is shown in figure 3 to see the detail. Note the small range in the horizontal and vertical coordinates.

The final cloud lies very near the equator. There is a a spread of about 30^o along the equator and a very small spread perpendicular to the equator. With a suitable blow-up of the latitude axis, a figure similar to Figure 3 would be obtained.

Note that $\hat{\kappa} = 1.69e10$ and $\hat{\kappa}_e + 2\hat{\dot{\delta}} = 1.78e10$ are approximately equal and are very large, reflecting the fact that the distribution is initially concentrated and isotropic. At the end of the 14 day propagation the distribution has become elongated along a great circle, with very small uncertainty in the projected cross-track direction. This is what one generally expects in orbital uncertainty propagation, where the uncertainty grows in the in-track direction. Future work on this example will focus on adding a terrestrial angles-only sensor and instead of just propagating the uncertainty, we will implement a modified UKF that employs an FB5e-based sensor error statistics. We will then use such a filter to better predict a space object's location into the future.

VII. Conclusion

The paper has reviewed the Fisher-Bingham distribution on the sphere and a variety of its special cases. A new special case, the extreme 5-parameter Fisher-Bingham distribution (FB5e) has been introduced to model semi-concentrated data on the sphere, where the distribution is unimodal but spread out close to a great circle. Recent advances in simulation and estimation for all the Fisher Bingham distributions have been summarized.

The motivation for FB5e comes from space tracking, where it is not unusual for distribution of the predicted angular location of a space object to have a a semi-concentrated form. Two simple examples have been given to illustrate the potential usefulness of FB5e. Work is underway to extend the analysis to more realistic orbital models.

ACKNOWLEDGMENT

This material is based upon work supported by the Air Force Office of Scientific Research, Air Force Material Command, USAF under Award No. FA9550-16-1-0099.

REFERENCES

[1] G. Kurz, I. Gilitschenski, S. Julier, and U. D. Hanebeck, "Recursive estimation of orientation based on the bingham distribution," in *Information Fusion (FUSION), 16th International Conference on*, 2013, pp. 1487–1494.

[2] J. L. Junkins, M. R. Akella, and K. T. Alfriend, "Non-Gaussian error propagation in orbital mechanics," *Journal of the Astronautical Sciences*, vol. 44, pp. 541–563, 1996.

[3] K. Fujimoto, D. J. Scheeres, and K. T. Alfriend, "Analytical nonlinear propagation of uncertainty in the two-body problem," *Journal of Guidance, Control, and Dynamics*, vol. 35, pp. 497–509, 2012.

[4] J. M. Aristoff, J. T. Horwood, and A. B. Poore, "Implicit Runge-Kutta methods for uncertainty propagation," in *Proceedings of the Advanced Maui Optical and Space Surveillance Technologies Conference, Wailea, HI, September 11–14*, 2012.

[5] J. T. Horwood and A. B. Poore, "Orbital state uncertainty realism," in *Proceedings of the Advanced Maui Optical and Space Surveillance Technologies Conference, Wailea, HI, September 11–14*, 2012.

[6] M. Valli, R. Armellin, P. D. Lizia, and M. R. Lavagna, "Nonlinear mapping of uncertainties in celestial mechanics," *Journal of Guidance, Control, and Dynamics*, vol. 36, pp. 48–63, 2013.

[7] G. Terejanu, P. Singla, T. Singh, and P. D. Scott, "Uncertainty propagation for nonlinear dynamics systems using Gaussian mixture models," *Journal of Guidance, Control, and Dynamics*, vol. 31, pp. 1623–1633, 2008.

[8] J. T. Horwood, N. D. Aragon, and A. B. Poore, "Gaussian sum filters for space surveillance: Theory and simulations," *Journal of Guidance, Control, and Dynamics*, vol. 34, pp. 1839–1851, 2011.

[9] K. J. DeMars, R. H. Bishop, and M. K. Jah, "A splitting Gaussian mixture method for the propagation of uncertainty in orbital mechanics," *Advances in the Astronautical Sciences*, vol. 140, 2012, (Proceedings of the 21st AAS/AIAA Spaceflight Mechanics Meeting, New Orleans, LA, February 13–17 2011, Paper AAS 11-201).

[10] Y. Cheng, K. J. DeMars, C. Früh, and M. K. Jah, "Gaussian mixture PHD filter for space object tracking," *Advances in the Astronautical Sciences*, vol. 148, pp. 649–668, 2013, (Proceedings of the 23rd AAS/AIAA Space Flight Mechanics Meeting, Kauai, HI, February 10–14 2013, Paper 13-242).

[11] J. T. Kent, "The Fisher-Bingham distribution on the sphere," *Journal of the Royal Statistical Society, Series B*, vol. 44, pp. 71–80, 1982.

[12] J. T. Kent, A. M. Ganeiber, and K. V. Mardia, "A new method to simulate the Bingham and related distributions in directional data analysis with applications," *ArXiv e-prints*, Oct. 2013.

[13] K. V. Mardia and P. E. Jupp, *Directional Statistics*. Chichester: Wiley, 2000.

[14] Y. Chikuse, *Statistics on Special Manifolds*. New York: Springer-Verlag, 2003.

[15] J. T. Kent and T. Hamelryck, "Using the Fisher-Bingham distribution in stochastic models for protein structure," in *Proceedings in Quantitative Biology, Shape Analysis and Wavelets*, S. Barber, P. D. Baxter, K. V. Mardia, and R. E. Walls, Eds. Leeds University Press, 2005, pp. 57–60.

[16] J. T. Kent, "Statistical modelling and simulation using the Fisher-Bingham distribution," in *Bayesian Methods in Structural Bioinformatics*, ser. Statistics for Biology and Health, T. Hamelryck, K. Mardia, and J. Ferkinghoff-Borg, Eds. Berlin: Springer-Verlag, 2012, pp. 179–188.

[17] ——, "Asymptotic expansions for the Bingham distribution," *Applied Statistics*, vol. 36, pp. 139–144, 1987.

[18] K. V. Mardia, J. T. Kent, and A. K. Laha, "Score matching estimators for directional distributions," *ArXiv e-prints*, April 2016.

[19] A. Hyvärinen, "Estimation of non-normalized statistical models by score matching," *Journal of Machine Learning Research*, vol. 6, pp. 695–709, 2005.

[20] ——, "Some extensions of score matching," *Computational Statistics & Data Analysis*, vol. 51, pp. 2499–2512, 2007.